

## Two-photon absorption spectroscopy of $\text{Cm}^{3+}$ in $\text{LuPO}_4$

K. M. Murdoch, A. D. Nguyen, and N. M. Edelstein

*Chemical Sciences Division, Lawrence Berkeley National Laboratory, Berkeley, California 94720*

S. Hubert

*Laboratoire de Radiochimie, Institut de Physique Nucléaire, Boîte Postale No. 1, 91406 Orsay, France*

J. C. Gâcon

*Laboratoire de Physico-Chimie des Matériaux Luminescents, UMR No. 5620 du CRNS et Université Lyon-I, 69622 Villeurbanne Cedex, France*

(Received 23 December 1996)

Laser excitation spectroscopy has been used to investigate two-photon absorption (TPA) transitions of the actinide ion  $\text{Cm}^{3+}$  in a  $\text{LuPO}_4$  host crystal. One-color two-photon excitation spectra were recorded in the energy ranges corresponding to the  ${}^8S_{7/2} \rightarrow {}^6D_{7/2}$  (16 400–17 200  $\text{cm}^{-1}$ ),  ${}^8S_{7/2} \rightarrow {}^6P_{5/2}$  (19 700–20 300  $\text{cm}^{-1}$ ), and  ${}^8S_{7/2} \rightarrow {}^6D_{7/2}$  (27 700–28 100  $\text{cm}^{-1}$ ) absorption transitions. The relative intensities and polarization dependences of the lines observed were measured. These results are compared to calculated intensities derived from the second-order theory of Axe and also from the second-order theory extended to include a third-order spin-orbit correction. There was poor agreement between experiment and theory for most of the TPA transitions investigated. Inclusion of an additional phenomenological imaginary term in the amplitude improved the agreement for these transitions. [S0163-1829(97)02429-6]

### I. INTRODUCTION

The optical properties of the  $\text{Cm}^{3+}$  ion ( $[\text{Rn}]5f^7$ ) and, for comparison the  $\text{Gd}^{3+}$  ion ( $[\text{Xe}]4f^7$ ), diluted in  $\text{LuPO}_4$  crystals, have been extensively investigated by one-photon laser spectroscopy.<sup>1,2,3</sup> The main differences in their optical properties arise from smaller values of the Slater parameters and the much larger spin-orbit interaction for  $\text{Cm}^{3+}$  as compared to  $\text{Gd}^{3+}$ . In addition, the crystal-field splittings are about a factor of 2 larger for the excited states of  $\text{Cm}^{3+}$  than for  $\text{Gd}^{3+}$  in the  $\text{LuPO}_4$  host crystal. The larger intermediate coupling for the  $\text{Cm}^{3+}$  ion results in a ground-term wave function which is only about 80%  ${}^8S_{7/2}$ , compared to the almost 100%  ${}^8S_{7/2}$  character of the ground-term wave function of the  $\text{Gd}^{3+}$  ion. As a consequence, the measured overall splitting of this nominally  ${}^8S_{7/2}$  ground multiplet is 9.5  $\text{cm}^{-1}$  for  $\text{Cm}^{3+}$  in  $\text{LuPO}_4$ .<sup>2,3</sup> It is therefore possible to distinguish absorption transitions originating from different levels of the  $\text{Cm}^{3+}$  ground multiplet spectroscopically and so measure their polarization behavior. Studies of other  $S$ -state ions, such as  $\text{Gd}^{3+}$  (Refs. 4–7) and  $\text{Eu}^{2+}$  (Ref. 8), have measured only the integrated intensities of two-photon absorption (TPA) transitions from their weakly split (less than 1  $\text{cm}^{-1}$ )  ${}^8S_{7/2}$  ground multiplet.

Analyses of the  ${}^8S_{7/2} \rightarrow {}^6P_J$  ( $J=3/2, 5/2, 7/2$ ) two-photon absorption transitions of  $\text{Gd}^{3+}$  ions in various host crystals have generated much theoretical interest since the standard second-order theory of Axe<sup>9</sup> has proved inadequate to explain their observed relative intensities.<sup>4–7</sup> Higher-order corrections involving the spin-orbit and/or crystal-field interactions between intermediate states, particularly those of the  $4f^6-5d$  lowest-lying excited configuration, were introduced to account for the observed discrepancies.<sup>10,11</sup> In the case of the  $\text{Cm}^{3+}$  ion, the relatively large admixtures of other SLJ states into the ground-term wave function by spin-orbit cou-

pling means the second-order intensity theory is more applicable, and so Axe's theory may better account for the TPA intensities. It is also possible that the large spin-orbit interaction will enhance the third-order contributions to the TPA intensities. In this paper we present the results of an experimental study of TPA transitions for  $\text{Cm}^{3+}$  in  $\text{LuPO}_4$ , including measurements of their relative intensities and polarization dependencies. These data are analyzed in terms of a new formalism which includes second- and third-order contributions.<sup>12</sup>

In this paper multiplets will be labeled according to their largest  ${}^{2S+1}L_J$  component. It follows from crystal-field analyses<sup>2,3</sup> that the first excited multiplet of the  $\text{Cm}^{3+}$  ion in  $\text{LuPO}_4$  is labeled  ${}^6D_{7/2}$  instead of  ${}^6P_{7/2}$  as in the case of the  $\text{Gd}^{3+}$  ion. The other  ${}^6D_{7/2}$  multiplet considered in this paper will be labeled  ${}^6D'_{7/2}$  to avoid ambiguity. The nomenclature  ${}^{2S+1}L_J(n)$  will be used to denote the  $n$ th highest-energy crystal-field level in a multiplet  ${}^{2S+1}L_J$ . The levels and wave functions are given in Table I.

### II. EXPERIMENT

Single crystals of  $\text{LuPO}_4$  doped with almost isotopically pure  ${}^{248}\text{Cm}$  were grown at Oak Ridge National Laboratory using the high-temperature solution technique described previously.<sup>13,14</sup> The crystal used for this study was relatively small, with dimensions of  $0.5 \times 2.0 \times 1.0 \text{ mm}^3$ . The nominal  $\text{Cm}^{3+}$  concentration is estimated to be less than 0.1 mol %. This radioactive sample was sealed in a quartz ampoule under a partial pressure of helium for containment purposes.

All the experiments, unless otherwise stated, were conducted at a temperature of 4.2 K in an Oxford Instruments CF1204 optical cryostat. The actual sample temperature may be somewhat higher due to the absorption of laser energy. Resistive coils and an Oxford Instruments ITCV4 tempera-

TABLE I. Electronic wave functions for the crystal-field states of Cm<sup>3+</sup> ions in LuPO<sub>4</sub>. Only one of the two Kramers doublets for each level is listed. The parametrized Hamiltonian and the specific fitting procedure were described in Refs. 2 and 3.

Experimental energy (cm <sup>-1</sup> )	Assignment	Wave function
0.0	<sup>8</sup> S <sub>7/2</sub> (1)Γ <sub>7</sub>	-0.844 <sup>8</sup> S <sub>7/2</sub> (7/2) - 0.403 <sup>6</sup> P <sub>7/2</sub> (7/2) + 0.088 <sup>6</sup> D <sub>7/2</sub> (7/2) - 0.269 <sup>8</sup> S <sub>7/2</sub> (-1/2) - 0.129 <sup>6</sup> P <sub>7/2</sub> (-1/2) + 0.028 <sup>6</sup> D <sub>7/2</sub> (-1/2)
3.5	<sup>8</sup> S <sub>7/2</sub> (2)Γ <sub>6</sub>	0.808 <sup>8</sup> S <sub>7/2</sub> (5/2) + 0.386 <sup>6</sup> P <sub>7/2</sub> (5/2) - 0.085 <sup>6</sup> D <sub>7/2</sub> (5/2) + 0.363 <sup>8</sup> S <sub>7/2</sub> (-3/2) + 0.173 <sup>6</sup> P <sub>7/2</sub> (-3/2) - 0.038 <sup>6</sup> D <sub>7/2</sub> (-3/2)
8.1	<sup>8</sup> S <sub>7/2</sub> (3)Γ <sub>6</sub>	0.363 <sup>8</sup> S <sub>7/2</sub> (5/2) + 0.173 <sup>6</sup> P <sub>7/2</sub> (5/2) - 0.038 <sup>6</sup> D <sub>7/2</sub> (5/2) + 0.808 <sup>8</sup> S <sub>7/2</sub> (-3/2) + 0.386 <sup>6</sup> P <sub>7/2</sub> (-3/2) - 0.085 <sup>6</sup> D <sub>7/2</sub> (-3/2)
9.5	<sup>8</sup> S <sub>7/2</sub> (4)Γ <sub>7</sub>	-0.269 <sup>8</sup> S <sub>7/2</sub> (7/2) - 0.129 <sup>6</sup> P <sub>7/2</sub> (7/2) + 0.028 <sup>6</sup> D <sub>7/2</sub> (7/2) - 0.844 <sup>8</sup> S <sub>7/2</sub> (-1/2) - 0.403 <sup>6</sup> P <sub>7/2</sub> (-1/2) + 0.088 <sup>6</sup> D <sub>7/2</sub> (-1/2)
16 528	<sup>6</sup> D <sub>7/2</sub> (1)Γ <sub>7</sub>	0.233 <sup>8</sup> S <sub>7/2</sub> (7/2) - 0.252 <sup>6</sup> P <sub>7/2</sub> (7/2) + 0.269 <sup>6</sup> D <sub>7/2</sub> (7/2) + 0.225 <sup>8</sup> S <sub>7/2</sub> (-1/2) - 0.244 <sup>6</sup> P <sub>7/2</sub> (-1/2) + 0.260 <sup>6</sup> D <sub>7/2</sub> (-1/2)
16 577	<sup>6</sup> D <sub>7/2</sub> (2)Γ <sub>6</sub>	0.307 <sup>8</sup> S <sub>7/2</sub> (5/2) - 0.332 <sup>6</sup> P <sub>7/2</sub> (5/2) + 0.354 <sup>6</sup> D <sub>7/2</sub> (5/2) + 0.104 <sup>8</sup> S <sub>7/2</sub> (-3/2) - 0.113 <sup>6</sup> P <sub>7/2</sub> (-3/2) + 0.121 <sup>6</sup> D <sub>7/2</sub> (-3/2)
16 945	<sup>6</sup> D <sub>7/2</sub> (3)Γ <sub>7</sub>	0.225 <sup>8</sup> S <sub>7/2</sub> (7/2) - 0.244 <sup>6</sup> P <sub>7/2</sub> (7/2) + 0.260 <sup>6</sup> D <sub>7/2</sub> (7/2) - 0.233 <sup>8</sup> S <sub>7/2</sub> (-1/2) + 0.252 <sup>6</sup> P <sub>7/2</sub> (-1/2) - 0.269 <sup>6</sup> D <sub>7/2</sub> (-1/2)
17 122	<sup>6</sup> D <sub>7/2</sub> (4)Γ <sub>6</sub>	0.104 <sup>8</sup> S <sub>7/2</sub> (5/2) - 0.113 <sup>6</sup> P <sub>7/2</sub> (5/2) + 0.120 <sup>6</sup> D <sub>7/2</sub> (5/2) - 0.306 <sup>8</sup> S <sub>7/2</sub> (-3/2) + 0.332 <sup>6</sup> P <sub>7/2</sub> (-3/2) - 0.354 <sup>6</sup> D <sub>7/2</sub> (-3/2)
19 778	<sup>6</sup> P <sub>5/2</sub> (1)Γ <sub>6</sub>	0.449 <sup>6</sup> P <sub>5/2</sub> (5/2) - 0.389 <sup>6</sup> D <sub>5/2</sub> (5/2) + 0.158 <sup>6</sup> F <sub>5/2</sub> (5/2) + 0.152 <sup>4</sup> D <sub>6<sub>5/2</sub></sub> (5/2) + 0.462 <sup>6</sup> P <sub>5/2</sub> (-3/2) - 0.400 <sup>6</sup> D <sub>5/2</sub> (-3/2) + 0.163 <sup>6</sup> F <sub>5/2</sub> (-3/2) + 0.157 <sup>4</sup> D <sub>6<sub>5/2</sub></sub> (-3/2)
20 017	<sup>6</sup> P <sub>5/2</sub> (2)Γ <sub>7</sub>	-0.621 <sup>6</sup> P <sub>5/2</sub> (-1/2) + 0.539 <sup>6</sup> D <sub>5/2</sub> (-1/2) - 0.219 <sup>6</sup> F <sub>5/2</sub> (-1/2) - 0.211 <sup>4</sup> D <sub>6<sub>5/2</sub></sub> (-1/2) - 0.028 <sup>6</sup> P <sub>7/2</sub> (7/2) + 0.030 <sup>6</sup> D <sub>7/2</sub> (7/2) - 0.038 <sup>8</sup> S <sub>7/2</sub> (-1/2) + 0.059 <sup>6</sup> P <sub>7/2</sub> (-1/2) + 0.062 <sup>6</sup> D <sub>7/2</sub> (-1/2)
20 181	<sup>6</sup> P <sub>5/2</sub> (3)Γ <sub>6</sub>	-0.442 <sup>6</sup> P <sub>5/2</sub> (5/2) + 0.384 <sup>6</sup> D <sub>5/2</sub> (5/2) - 0.156 <sup>6</sup> F <sub>5/2</sub> (5/2) - 0.150 <sup>4</sup> D <sub>6<sub>5/2</sub></sub> (5/2) + 0.446 <sup>6</sup> P <sub>5/2</sub> (-3/2) - 0.387 <sup>6</sup> D <sub>5/2</sub> (-3/2) + 0.157 <sup>6</sup> F <sub>5/2</sub> (-3/2) + 0.152 <sup>4</sup> D <sub>6<sub>5/2</sub></sub> (-3/2)
27 875	<sup>6</sup> D' <sub>7/2</sub> (1)Γ <sub>6</sub>	-0.050 <sup>6</sup> P <sub>7/2</sub> (5/2) - 0.063 <sup>6</sup> D <sub>7/2</sub> (5/2) + 0.052 <sup>6</sup> F <sub>7/2</sub> (5/2) - 0.041 <sup>6</sup> G <sub>7/2</sub> (5/2) - 0.039 <sup>4</sup> D <sub>6<sub>7/2</sub></sub> (5/2) - 0.029 <sup>4</sup> D <sub>1<sub>7/2</sub></sub> (5/2) + 0.360 <sup>6</sup> P <sub>7/2</sub> (-3/2) + 0.457 <sup>6</sup> D <sub>7/2</sub> (-3/2) - 0.378 <sup>6</sup> F <sub>7/2</sub> (-3/2) + 0.299 <sup>6</sup> G <sub>7/2</sub> (-3/2) + 0.285 <sup>4</sup> D <sub>6<sub>7/2</sub></sub> (-3/2) + 0.213 <sup>4</sup> D <sub>1<sub>7/2</sub></sub> (-3/2)
27 899	<sup>6</sup> D' <sub>7/2</sub> (2)Γ <sub>7</sub>	0.187 <sup>6</sup> P <sub>7/2</sub> (7/2) + 0.238 <sup>6</sup> D <sub>7/2</sub> (7/2) - 0.197 <sup>6</sup> F <sub>7/2</sub> (7/2) + 0.155 <sup>6</sup> G <sub>7/2</sub> (7/2) + 0.148 <sup>4</sup> D <sub>6<sub>7/2</sub></sub> (7/2) + 0.111 <sup>4</sup> D <sub>1<sub>7/2</sub></sub> (7/2) - 0.305 <sup>6</sup> P <sub>7/2</sub> (-1/2) - 0.387 <sup>6</sup> D <sub>7/2</sub> (-1/2) + 0.320 <sup>6</sup> F <sub>7/2</sub> (-1/2) - 0.252 <sup>6</sup> G <sub>7/2</sub> (-1/2) - 0.241 <sup>4</sup> D <sub>6<sub>7/2</sub></sub> (-1/2) - 0.180 <sup>4</sup> D <sub>1<sub>7/2</sub></sub> (-1/2)
27 998	<sup>6</sup> D' <sub>7/2</sub> (3)Γ <sub>6</sub>	-0.362 <sup>6</sup> P <sub>7/2</sub> (5/2) - 0.459 <sup>6</sup> D <sub>7/2</sub> (5/2) + 0.380 <sup>6</sup> F <sub>7/2</sub> (5/2) - 0.300 <sup>6</sup> G <sub>7/2</sub> (5/2) - 0.286 <sup>4</sup> D <sub>6<sub>7/2</sub></sub> (5/2) - 0.214 <sup>4</sup> D <sub>1<sub>7/2</sub></sub> (5/2) - 0.056 <sup>6</sup> P <sub>7/2</sub> (-3/2) - 0.071 <sup>6</sup> D <sub>7/2</sub> (-3/2) + 0.058 <sup>6</sup> F <sub>7/2</sub> (-3/2) - 0.046 <sup>6</sup> G <sub>7/2</sub> (-3/2) - 0.044 <sup>4</sup> D <sub>6<sub>7/2</sub></sub> (-3/2) - 0.033 <sup>4</sup> D <sub>1<sub>7/2</sub></sub> (-3/2)
28 022	<sup>6</sup> D' <sub>7/2</sub> (4)Γ <sub>7</sub>	-0.298 <sup>6</sup> P <sub>7/2</sub> (7/2) - 0.378 <sup>6</sup> D <sub>7/2</sub> (7/2) + 0.313 <sup>6</sup> F <sub>7/2</sub> (7/2) - 0.247 <sup>6</sup> G <sub>7/2</sub> (7/2) - 0.235 <sup>4</sup> D <sub>6<sub>7/2</sub></sub> (7/2) - 0.176 <sup>4</sup> D <sub>1<sub>7/2</sub></sub> (7/2) - 0.200 <sup>6</sup> P <sub>7/2</sub> (-1/2) - 0.254 <sup>6</sup> D <sub>7/2</sub> (-1/2) + 0.210 <sup>6</sup> F <sub>7/2</sub> (-1/2) - 0.166 <sup>6</sup> G <sub>7/2</sub> (-1/2) - 0.158 <sup>4</sup> D <sub>6<sub>7/2</sub></sub> (-1/2) - 0.118 <sup>4</sup> D <sub>1<sub>7/2</sub></sub> (-1/2)

ture controller were sometimes used to raise the sample temperature.

Initially TPA spectra of the  ${}^8S_{7/2} \rightarrow {}^6D_{7/2}$  transitions were obtained using a Nd:YAG pumped dye laser and a hydrogen Raman cell. Sulforhodamine B was an appropriate dye for the Stokes II shifted beam. Other Stokes and anti-Stokes beams from the Raman shifter were stopped by two Schott RG 1000 color filters, one attached directly to the window of the cryostat. Moreover, a Pellin-Broca prism was used to spatially separate the desired excitation beam. This beam, of up to 4 mJ/pulse power, was focused onto the sample by a 21 cm lens. Its polarization was set using an Optics for Research SB-10 Soleil Babinet compensator. The photomultiplier tube housing was attached directly to the cryostat, with a single 5-cm lens to collect the  $\text{Cm}^{3+}$  fluorescence and direct it onto the photocathode. A Schott 605 21-nm interference filter was placed in front of this lens to eliminate scattered laser light and select the overall  ${}^6D_{7/2} \rightarrow {}^8S_{7/2}$  fluorescence. The signal was measured with a Princeton Applied Research 162 boxcar averager, with a gate width of 1 ms. The  ${}^6D_{7/2}(1)$  emitting level has a fluorescence lifetime of  $(580 \pm 60) \mu\text{s}$ .<sup>2</sup>

To confirm these results, the experiment was repeated using a Lambda Physik Scanmate optical parametric oscillator (OPO) as the excitation source. This is a hybrid OPO, which uses a small dye oscillator as a seed laser. It was pumped by the third-harmonic output of a Spectra Physics GCR-3 Nd:YAG laser. The output beam was passed through a Corning 2-64 color filter. It had a sufficiently broad transverse mode for a Spectra Physics 310-21 polarization rotator to be used to change the excitation polarization. The polarization of the transmitted excitation beam was checked and found to be linear, confirming that there was no depolarization caused by birefringence in either the sample or the cryostat windows. The excitation power was usually 600  $\mu\text{J}/\text{pulse}$  and was never increased above 1 mJ/pulse. A 25-cm quartz lens was used to focus the beam onto the crystal. A Hamamatsu IP28 photomultiplier tube was placed against the window of the cryostat to detect the  ${}^6D_{7/2} \rightarrow {}^8S_{7/2}$  fluorescence. A 2-73 color filter and a 602 10-nm line filter were placed between them. The signal was amplified by a Stanford Research SR445 fast preamplifier and then measured using a Stanford Research model SR400 gated photon counter, with a gate delay of 10  $\mu\text{s}$  and width of 2 ms. Neutral density filters were used to avoid pulse pileup with strong signals.

This same setup was used to observe the  ${}^8S_{7/2} \rightarrow {}^6P_{5/2}$  TPA transitions. TPA to the  ${}^6D_{7/2}$  multiplet was observed in the same way, but using a Spectra Physics PDL-3 dye laser with LDS750 dye as the excitation source.

Transition intensities were measured from the TPA spectra using the line fitting routines of the GRAMS/386 program from Galactic Industries. Initially all the lines in a spectral region were fitted to Lorentzian functions, without constraining the fitting parameters, to establish the position and width of each line. For the final fits to determine the line areas, both these parameters were fixed, and just the peak intensities were fitted. Experimental uncertainties were estimated from the reproducibility of transition intensities measured from different spectra which were obtained under identical experimental conditions. For the transitions investigated here, the uncertainties for the final line areas were approxi-

mately 5% for the excitation polarizations corresponding to the peak absorption intensity.

### III. THEORETICAL

The  $\text{LuPO}_4$  host lattice has tetragonal zircon-type structure with the space-group  $D_{4h}^{19}$ . The  $\text{Cm}^{3+}$  ions enter the lattice substitutionally for  $\text{Lu}^{3+}$  ions at sites of  $D_{2d}$  point symmetry.<sup>1</sup> The polarization of incident photons is described in polar coordinates with respect to the  $\text{Cm}^{3+}$  site axes. The  $z$  axis is parallel to the crystallographic  $c$  axis,  $\theta$  is the angle between the polarization unit vector and the  $z$  axis, and  $\varphi$  is the angle between the polarization unit vector and the  $x$  axis in the  $x$ - $y$  plane. In  $\text{LuPO}_4$  the  $\text{Cm}^{3+}$  site axes are rotated by  $45^\circ$  about the  $z$  axis from the crystallographic axes.<sup>6</sup> Therefore the angle  $\varphi$  is  $45^\circ$  for a beam entering the crystal normal to one of the cleavage faces.

The theoretical analysis of the polarization-dependent behavior of  $\text{Cm}^{3+}$  ions in  $\text{LuPO}_4$  follows the general formalism for the intensities of two-photon transitions developed by Nguyen.<sup>12</sup> The one-color two-photon transition intensity between an initial state  $|i\rangle$  and a final state  $|f\rangle$  is proportional to

$$S_{if} = |\langle i | \alpha_{\text{TPA}} | f \rangle|^2, \quad (1)$$

where  $\alpha_{\text{TPA}}$  is the two-photon tensor operator:<sup>12</sup>

$$\begin{aligned} \alpha_{\text{TPA}} = & \frac{-1}{\sqrt{3}} \alpha_0^{(0)} + \frac{3 \cos^2 \theta - 1}{\sqrt{6}} \alpha_0^{(2)} - \frac{e^{-i\varphi} \sin 2\theta}{2} \alpha_1^{(2)} \\ & + \frac{e^{i\varphi} \sin 2\theta}{2} \alpha_{-1}^{(2)} + \frac{e^{-2i\varphi} \sin^2 \theta}{2} \alpha_2^{(2)} + \frac{e^{2i\varphi} \sin^2 \theta}{2} \alpha_{-2}^{(2)}. \end{aligned} \quad (2)$$

In the second-order approximation, the irreducible tensors  $\alpha_q^{(t)}$  are related to the spherical tensors  $U_k^{(t)}$  by

$$(\alpha_q^{(t)})^{2\text{nd}} = F_t U_q^{(t)}, \quad (3)$$

where

$$\begin{aligned} F_t = & (-1)^t \sum_{n'l'} 7(2l'+1) \begin{pmatrix} 3 & 1 & l' \\ 0 & 0 & 0 \end{pmatrix}^2 \langle 5f | \mathbf{r} | n'l' \rangle^2 \\ & \times (2t+1)^{1/2} \begin{Bmatrix} 1 & 3 & l' \\ 3 & 1 & t \end{Bmatrix} \left[ \frac{1}{E_{n'l'} - \hbar\omega} \right]. \end{aligned} \quad (4)$$

$E_{n'l'}$  is defined as the average energy of the  $5f^6 n'l'$  configuration above the  $5f^7$  ground level and  $\hbar\omega$  is the energy of each incident photon. Expressing the initial and final crystal-field states in terms of Russell-Saunders coupled wave functions

$$|i\rangle = \sum_{\alpha SLJ_z} a(i; 5f^7 \alpha SLJ_z) |5f^7 \alpha SLJ_z\rangle, \quad (5)$$

$$|f\rangle = \sum_{\alpha' S' L' J' J'_z} a'(f; 5f^7 \alpha' S' L' J' J'_z) |5f^7 \alpha' S' L' J' J'_z\rangle,$$

the contribution of the second-order matrix element of the spherical irreducible tensor  $\alpha_q^{(t)}$  is given by:

$$\langle i | \alpha_q^{(t)} | f \rangle = F_l \sum_{\alpha SLJJ_z} \sum_{\alpha' S' L' J' J'_z} a(i; 5f^7 \alpha SLJJ_z) a'(f; 5f^7 \alpha' S' L' J' J'_z) \langle 5f^7 \alpha SLJJ_z | \mathbf{U}_q^{(t)} | 5f^7 \alpha' S' L' J' J'_z \rangle, \quad (6)$$

where

$$\begin{aligned} & \langle 5f^7 \alpha SLJJ_z | \mathbf{U}_q^{(t)} | 5f^7 \alpha' S' L' J' J'_z \rangle \\ &= (-1)^{2J+S+L'+t-J_z} [(2J+1)(2J'+1)]^{1/2} \begin{pmatrix} J & t & J' \\ -J_z & q & J'_z \end{pmatrix} \begin{Bmatrix} J & t & J' \\ L' & S & L \end{Bmatrix} \langle 5f^7 \alpha SL || U^{(t)} || 5f^7 \alpha' S L' \rangle \delta(S, S') \end{aligned} \quad (7)$$

and  $\mathbf{U}^{(t)}$  is the many-electron Racah unit tensor of orbital rank  $t$ .

The third-order contributions, taking into account spin-orbit interactions within the lowest-lying excited configuration  $5f^6 6d$ , are given by<sup>12</sup>

$$\begin{aligned} & \langle 5f^7 \alpha SLJJ_z | (\alpha_0^{(0)})^{3rd} | 5f^7 \alpha' S' L' J' J'_z \rangle \\ &= \left[ \sqrt{\frac{7}{2}} H(0) - G(0,1) \right] (2J+1)^{-1/2} \langle 5f^7 \alpha SLJ || \mathbf{W}^{(11)0} || 5f^7 \alpha' S' L' J \rangle \delta(J, J') \delta(J_z, J'_z) \end{aligned} \quad (8)$$

and

$$\begin{aligned} & \langle 5f^7 \alpha SLJJ_z | (\alpha_q^{(2)})^{3rd} | 5f^7 \alpha' S' L' J' J'_z \rangle = (-1)^{J-J_z} \begin{pmatrix} J & 2 & J' \\ -J_z & q & J'_z \end{pmatrix} \left[ \sqrt{\frac{5}{2}} H(2) (2J'+1)^{-1/2} \right. \\ & \quad \times \sum_{\alpha'' L''} \langle 5f^7 \alpha SLJ || \mathbf{U}^{(2)} || 5f^7 \alpha'' S L'' J'' \rangle \langle 5f^7 \alpha'' S L'' J'' || \mathbf{W}^{(11)0} || 5f^7 \alpha' S' L' J' \rangle \\ & \quad - G(2,1) \langle 5f^7 \alpha SLJ || \mathbf{W}^{(11)2} || 5f^7 \alpha' S' L' J' \rangle - G(2,2) \\ & \quad \left. \times \langle 5f^7 \alpha SLJ || \mathbf{W}^{(12)2} || 5f^7 \alpha' S' L' J' \rangle - G(2,3) \langle 5f^7 \alpha SLJ || \mathbf{W}^{(13)2} || 5f^7 \alpha' S' L' J' \rangle \right], \end{aligned} \quad (9)$$

where  $\mathbf{W}^{(1\lambda)t}$  is a double tensor of spin rank 1, orbital rank 2, and total rank  $t$ .  $H(t)$  and  $G(t, \lambda)$  are defined as follows:

$$\begin{aligned} H(0) &= \frac{6\zeta_f}{(E_{6d} - \hbar\omega)^2} (5f|r|6d)^2, & G(0,1) &= \frac{(6\zeta_f - 4\zeta_d)}{\sqrt{14}(E_{6d} - \hbar\omega)^2} (5f|r|6d)^2, \\ H(2) &= \frac{6\sqrt{6}\zeta_f}{5(E_{6d} - \hbar\omega)^2} (5f|r|6d)^2, & G(2,1) &= \frac{(-18\zeta_f + 8\zeta_d)}{\sqrt{1400}(E_{6d} - \hbar\omega)^2} (5f|r|6d)^2, \\ G(2,2) &= \frac{-3\sqrt{42}\zeta_f}{70(E_{6d} - \hbar\omega)^2} (5f|r|6d)^2, & G(2,3) &= \frac{3\sqrt{42}(\zeta_f - \zeta_d)}{35(E_{6d} - \hbar\omega)^2} (5f|r|6d)^2. \end{aligned} \quad (10)$$

Symmetry selection rules for a given  $\Gamma_i \rightarrow \Gamma_f$  transition between two Stark levels of symmetries  $\Gamma_i$  and  $\Gamma_f$  lead to specific expressions for the  $\alpha_{\text{TPA}}$  operator. This operator has even parity, and the  $\alpha^{(t)}$  tensors are irreducible tensor operators transforming as the  $D_t^+$  irreducible representation of the full rotation group. When considering the  $D_{2d}$  group, the  $\alpha^{(t)}$  tensors can be expressed as a sum of irreducible tensors  $\alpha_{\Gamma' \gamma'}^{(t)}$ :

$$\alpha_q^{(t)} = \sum_{\Gamma' \gamma'} \alpha_{\Gamma' \gamma'}^{(t)} (t \Gamma' \gamma' | tq). \quad (11)$$

These tensors transform as the irreducible representations  $\Gamma'$  of the group  $D_{2d}$ , appearing in the reduction of  $D_t^+$ . The additional  $\gamma'$  index is necessary when  $\Gamma'$  has a dimension greater than unity. The  $(t \Gamma' \gamma' | tq)$  coefficients have already been calculated for the  $C_{4v}$  group,<sup>15</sup> which is isomorphic to  $D_{2d}$ . Specifically, the relevant tensors are

$$\alpha_0^{(t)} = \alpha_{\Gamma_1}^{(t)} \quad (\text{where } t=0,2),$$

$$\alpha_{\pm 1}^{(2)} = \frac{\pm 1}{\sqrt{2}} (\alpha_{\Gamma_5 \gamma_1}^{(2)} \pm \alpha_{\Gamma_5 \gamma_2}^{(2)}),$$

TABLE II. Effective tensor operators for two-photon transitions of  $\text{Cm}^{3+}$  ions in  $D_{2d}$  symmetry.

Transition	Operator
$\Gamma_6 \leftrightarrow \Gamma_6$	$\alpha_{\text{TPA}} = -\frac{1}{\sqrt{3}} \alpha_0^{(0)} + \frac{3 \cos^2 \theta - 1}{\sqrt{6}} \alpha_0^{(2)}$ $- \frac{e^{-i\varphi} \sin 2\theta}{2} \alpha_1^{(2)} + \frac{e^{i\varphi} \sin 2\theta}{2} \alpha_{-1}^{(2)}$
$\Gamma_7 \leftrightarrow \Gamma_7$	$\alpha_{\text{TPA}} = -\frac{1}{\sqrt{3}} \alpha_0^{(0)} + \frac{3 \cos^2 \theta - 1}{\sqrt{6}} \alpha_0^{(2)}$ $- \frac{e^{-i\varphi} \sin 2\theta}{2} \alpha_1^{(2)} + \frac{e^{i\varphi} \sin 2\theta}{2} \alpha_{-1}^{(2)}$
$\Gamma_6 \leftrightarrow \Gamma_7$	$\alpha_{\text{TPA}} = -\frac{e^{-i\varphi} \sin 2\theta}{2} \alpha_1^{(2)} + \frac{e^{i\varphi} \sin 2\theta}{2} \alpha_{-1}^{(2)}$ $+ \frac{e^{-2i\varphi} \sin^2 \theta}{2} \alpha_2^{(2)} + \frac{e^{2i\varphi} \sin^2 \theta}{2} \alpha_{-2}^{(2)}$

$$\alpha_{\pm 2}^{(2)} = \frac{1}{\sqrt{2}} (\alpha_{\Gamma_3}^{(2)} \pm \alpha_{\Gamma_4}^{(2)}). \quad (12)$$

It follows that the nonvanishing contributions to  $\Gamma_6 \rightarrow \Gamma_6$  or  $\Gamma_7 \rightarrow \Gamma_7$  TPA transitions between the Kramers doublet levels will involve only the  $\alpha_0^{(i)}$  and  $\alpha_{\pm 1}^{(2)}$  matrix elements, whereas only the  $\alpha_{\pm 1}^{(2)}$  and  $\alpha_{\pm 2}^{(2)}$  elements will contribute to  $\Gamma_6 \leftrightarrow \Gamma_7$  TPA transitions (Table II). A consequence is that the  $\Gamma_6 \rightarrow \Gamma_6$  and  $\Gamma_7 \rightarrow \Gamma_7$  transitions will be more sensitive to third-order corrections, as the  $\alpha_0^{(0)}$  contribution is zero in the second order.

The crystal-field wave functions for  $\text{Cm}^{3+}$  in  $\text{LuPO}_4$  for the levels investigated have been given in Table I. Only one state of the Kramers doublet is given for each level. These wave functions were calculated from the parameters of a phenomenological Hamiltonian, which had been fitted to 80 experimental energy levels.<sup>3</sup> Using the crystal-field wave functions given in Table I, the polarization dependences of the TPA intensities can be calculated. Only those  $2S+1L_J$  components greater than 1% were used in the calculations. The  $\alpha_q^t = \langle i | \alpha_q^{(t)} | f \rangle$  matrix elements were calculated up to

third order, and the nonzero values are listed in Table III. The polarization dependences of the TPA transitions investigated are given in Table IV.

## IV. RESULTS

### A. ${}^8S_{7/2} \rightarrow {}^6D_{7/2}$ transitions

Two-photon absorption was observed to three of the four levels of the  ${}^6D_{7/2}$  multiplet [Figs. 1(b) and 1(c)], Figure 1(a) shows the comparable single-photon absorption. Two transitions were observed to the  ${}^6D_{7/2}(1)$  level [Fig. 1(b)], which are separated by  $3.5 \text{ cm}^{-1}$ . This is a ground multiplet splitting and identifies these transitions unambiguously as originating from the two lowest  ${}^8S_{7/2}$  levels. The fitted linewidths are  $3.5 \text{ cm}^{-1}$ , broader than the  $2.3 \text{ cm}^{-1}$  inhomogeneous linewidths measured by single-photon absorption. Their measured and calculated polarization dependences are shown in Fig. 2. The polarization behavior is unusual in that both transitions are more isotropic than expected. At higher temperatures a third transition was seen, which originates from the third ground multiplet level. However, it was too weak to yield good line fits.

Two transitions were observed to the  ${}^6D_{7/2}(2)$  level, separated by  $7.9 \text{ cm}^{-1}$ , originating from the first and third ground multiplet levels. Just one broad line, with a linewidth of  $20.2 \text{ cm}^{-1}$ , was observed to the  ${}^6D_{7/2}(3)$  level [Fig. 1(c)]. The originating levels can not be determined definitively, as no ground-state splittings are resolved. However, the strong polarization anisotropy (Fig. 2) suggests that this transition comprises absorption from mainly one level. As the intensity of this line decreases immediately on heating the sample, this transition probably originates from the lowest ground multiplet level.

In addition to the electronic transitions, there are numerous minor excitation features in the spectra which have reproducible structure. These were also observed in single-photon absorption [Fig. 1(a)] and appear to be phonon bands coupled to the main electronic lines. Their displacements are in approximate agreement with phonon energies measured by Raman spectroscopy.<sup>16</sup> In the two-photon spectrum, the features in the region  $16\,800\text{--}16\,920 \text{ cm}^{-1}$  appear strongest when  $\theta = 90^\circ$ . This would suggest that they are coupled to the  ${}^8S_{7/2}(1) \rightarrow {}^6D_{7/2}(2)$  transition, which also appears strongly when  $\theta = 90^\circ$ .

TABLE III. Nonzero values of the  $\alpha_q^t$  parameters calculated for TPA transitions to the  ${}^6D_{7/2}$ ,  ${}^6P_{5/2}$ , and  ${}^6D'_{7/2}$  multiplets of  $\text{Cm}^{3+}$  in  $\text{LuPO}_4$  ( $\varphi = 45^\circ$ ).

Transition ( $\text{cm}^{-1}$ )	Second order ( $\alpha_q^t \times 10^{-7}$ )	Second and third order ( $\alpha_q^t \times 10^{-7}$ )
${}^8S_{7/2}(1) \rightarrow {}^6D_{7/2}(1)$	$\alpha_0^2 = 1.36$	$\alpha_0^2 = 1.93, \alpha_0^0 = 7.88$
${}^8S_{7/2}(2) \rightarrow {}^6D_{7/2}(1)$	$\alpha_2^2 = 0.655, \alpha_{-2}^2 = 1.67, \alpha_{\pm 1}^2 = 1.22$	$\alpha_2^2 = 0.929, \alpha_{-2}^2 = 2.36, \alpha_{\pm 1}^2 = 1.73$
${}^8S_{7/2}(1) \rightarrow {}^6D_{7/2}(2)$	$\alpha_2^2 = -0.226, \alpha_{-2}^2 = -0.989, \alpha_{\pm 1}^2 = 2.01$	$\alpha_2^2 = -0.321, \alpha_{-2}^2 = -1.41, \alpha_{\pm 1}^2 = 2.86$
${}^8S_{7/2}(1) \rightarrow {}^6D_{7/2}(3)$	$\alpha_0^2 = 2.09$	$\alpha_0^2 = 2.96, \alpha_0^0 = 3.91$
${}^8S_{7/2}(1) \rightarrow {}^6P_{5/2}(1)$	$\alpha_2^2 = 0.243, \alpha_{-2}^2 = -1.27, \alpha_{\pm 1}^2 = -0.960$	$\alpha_2^2 = 0.298, \alpha_{-2}^2 = -1.55, \alpha_{\pm 1}^2 = -1.18$
${}^8S_{7/2}(2) \rightarrow {}^6P_{5/2}(1)$	$\alpha_0^2 = 1.53, \alpha_{\pm 1}^2 = -0.568$	$\alpha_0^2 = 1.88, \alpha_{\pm 1}^2 = -0.697$
${}^8S_{7/2}(1) \rightarrow {}^6D'_{7/2}(1)$	$\alpha_2^2 = 0.559, \alpha_{-2}^2 = 0.968, \alpha_{\pm 1}^2 = -0.526$	$\alpha_2^2 = 0.710, \alpha_{-2}^2 = 1.23, \alpha_{\pm 1}^2 = 0.668$
${}^8S_{7/2}(2) \rightarrow {}^6D'_{7/2}(1)$	$\alpha_0^2 = 0.393, \alpha_{\pm 1}^2 = 1.59$	$\alpha_0^2 = 0.502, \alpha_0^0 = 2.03, \alpha_{\pm 1}^2 = 2.03$
${}^8S_{7/2}(1) \rightarrow {}^6D'_{7/2}(2)$	$\alpha_0^2 = 1.38$	$\alpha_0^2 = 1.76, \alpha_0^0 = -1.54$
${}^8S_{7/2}(2) \rightarrow {}^6D'_{7/2}(2)$	$\alpha_2^2 = 0.637, \alpha_{-2}^2 = 0.990, \alpha_{\pm 1}^2 = 1.21$	$\alpha_2^2 = 0.812, \alpha_{-2}^2 = 1.26, \alpha_{\pm 1}^2 = 1.54$

TABLE IV. Calculated polarization dependences of TPA intensities for transitions to the  ${}^6D_{7/2}$ ,  ${}^6P_{5/2}$ , and  ${}^6D'_{7/2}$  multiplets of  $\text{Cm}^{3+}$  in  $\text{LuPO}_4$  ( $\varphi=45^\circ$ ).

Transition ( $\text{cm}^{-1}$ )	Second order $ \alpha_{\text{TPA}} ^2 \times 10^{14}$	Second and third order $ \alpha_{\text{TPA}} ^2 \times 10^{14}$
${}^8S_{7/2}(1) \rightarrow {}^6D_{7/2}(1)$	$0.616 (3 \cos^2\theta - 1)^2$	$11.1 (2.26 - \cos^2\theta)^2$
${}^8S_{7/2}(2) \rightarrow {}^6D_{7/2}(1)$	$0.511 \sin^4\theta + 0.743 \sin^2 2\theta$	$\sin^4\theta + 1.50 \sin^2 2\theta$
${}^8S_{7/2}(1) \rightarrow {}^6D_{7/2}(2)$	$0.29 \sin^4\theta + 2.02 \sin^2 2\theta$	$0.58 \sin^4\theta + 4.09 \sin^2 2\theta$
${}^8S_{7/2}(1) \rightarrow {}^6D_{7/2}(3)$	$1.45 (3 \cos^2\theta - 1)^2$	$24.0 (1 - 1.06 \cos^2\theta)^2$
${}^8S_{7/2}(1) \rightarrow {}^6P_{5/2}(1)$	$1.14 \sin^4\theta + 0.46 \sin^2 2\theta$	$1.70 \sin^4\theta + 0.70 \sin^2 2\theta$
${}^8S_{7/2}(2) \rightarrow {}^6P_{5/2}(1)$	$0.784 (3 \cos^2\theta - 1)^2 + 0.161 \sin^2 2\theta$	$1.18 (3 \cos^2\theta - 1)^2 + 0.24 \sin^2 2\theta$
${}^8S_{7/2}(1) \rightarrow {}^6D'_{7/2}(1)$	$0.084 \sin^4\theta + 0.138 \sin^2 2\theta$	$0.135 \sin^4\theta + 0.224 \sin^2 2\theta$
${}^8S_{7/2}(2) \rightarrow {}^6D'_{7/2}(1)$	$0.05 (3 \cos^2\theta - 1)^2 + 1.26 \sin^2 2\theta$	$2.00 (0.61 \cos^2\theta - 1.38)^2 + 2.06 \sin^2 2\theta$
${}^8S_{7/2}(1) \rightarrow {}^6D'_{7/2}(2)$	$0.635 (3 \cos^2\theta - 1)^2$	$9.24 (\cos^2\theta + 0.080)^2$
${}^8S_{7/2}(2) \rightarrow {}^6D'_{7/2}(2)$	$0.062 \sin^4\theta + 0.732 \sin^2 2\theta$	$0.10 \sin^4\theta + 1.19 \sin^2 2\theta$

### B. ${}^8S_{7/2} \rightarrow {}^6P_{5/2}$ transitions

Two-photon absorption was observed to two of the three levels of the  ${}^6P_{5/2}$  multiplet (Fig. 3). Three distinct transitions can be discerned to the  ${}^6P_{5/2}(1)$  level. Two of these originate from the two lowest levels of the ground multiplet and are identified by their common splitting of  $3.1 \text{ cm}^{-1}$ . Their experimental and predicted polarization behaviors are shown in Fig. 4. The third transition could originate from either or both of the third and fourth ground multiplet levels, with a fitted displacement of  $8.8 \text{ cm}^{-1}$  from the  ${}^8S_{7/2}(1) \rightarrow {}^6P_{5/2}(1)$  transition. The line to the  ${}^6P_{5/2}(3)$  level could not be resolved into its ground-state components, and its shape and intensity do not change appreciably with temperature.

Phonon bands were also observed in these two-phonon excitation spectra. With the exception of the unidentified feature  $20 \text{ cm}^{-1}$  higher than the  ${}^8S_{7/2}(1) \rightarrow {}^6P_{5/2}(1)$  transition, these are weaker than for single-photon excitation.

### C. ${}^8S_{7/2} \rightarrow {}^6D'_{7/2}$ transitions

Two-photon absorption was observed to all four crystal field levels of the  ${}^6D'_{7/2}$  multiplet, Fig. 5. Two of the transitions to the  ${}^6D'_{7/2}(1)$  level could be identified as originating from the two lowest levels of the ground multiplet. There was an additional transition with a displacement of  $9.1 \text{ cm}^{-1}$ , which probably originated from one or both of the higher ground multiplet levels. These three transitions had fitted linewidths of  $4.8 \text{ cm}^{-1}$ . Similarly, both the transitions between the two lowest ground multiplet levels and the  ${}^6D'_{7/2}(2)$  level were identified. Again a third transition, with a displacement of  $8.6 \text{ cm}^{-1}$ , was also observed. The experimental and predicted polarization behaviors of these transitions are shown in Fig. 6.

A broad line was observed to each of the  ${}^6D'_{7/2}(3)$  and  ${}^6D'_{7/2}(4)$  levels. Neither of these could be resolved sufficiently to distinguish components originating from the different ground multiplet levels. Both of these exhibit rather isotropic polarization behavior. The excitation power dependence was measured for these two lines. In both cases there was a quadratic dependence, affirming their two-photon nature.

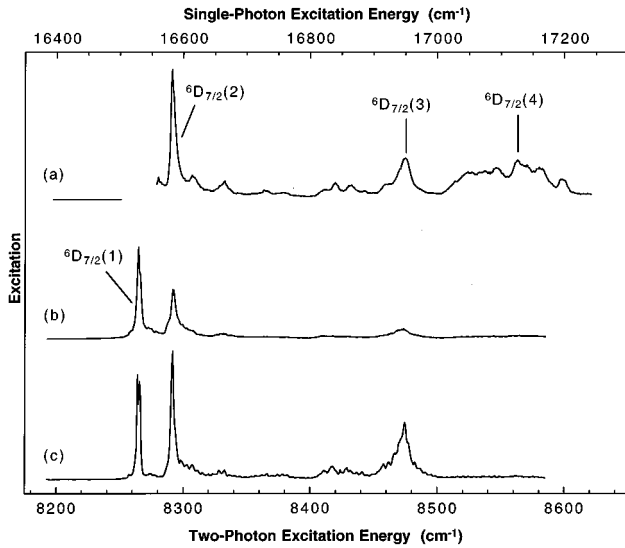


FIG. 1. (a)  $\theta=0^\circ$  polarized spectrum of the single-photon absorption transitions to the  ${}^6D_{7/2}$  multiplet. The single-photon excitation spectrum was interrupted near  $16525 \text{ cm}^{-1}$  to avoid damaging the photomultiplier tube, which was monitoring the overall  ${}^6D_{7/2} \rightarrow {}^8S_{7/2}$  fluorescence. (b)  $\theta=0^\circ$  and (c)  $\theta=90^\circ$  polarized spectra of the TPA transitions to the  ${}^6D_{7/2}$  multiplet obtained with the OPO.

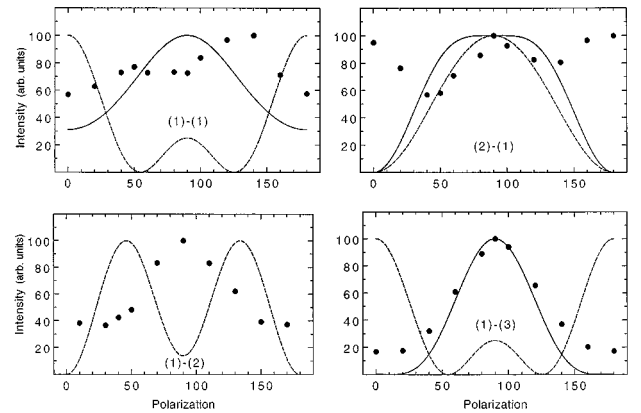


FIG. 2. Experimental polarization behavior (dots) of the  ${}^8S_{7/2} \rightarrow {}^6D_{7/2}$  two-photon absorption transitions. The second-order (dashed line) and combined second- and third-order (solid line) calculated polarization dependences are shown on different arbitrary scales.

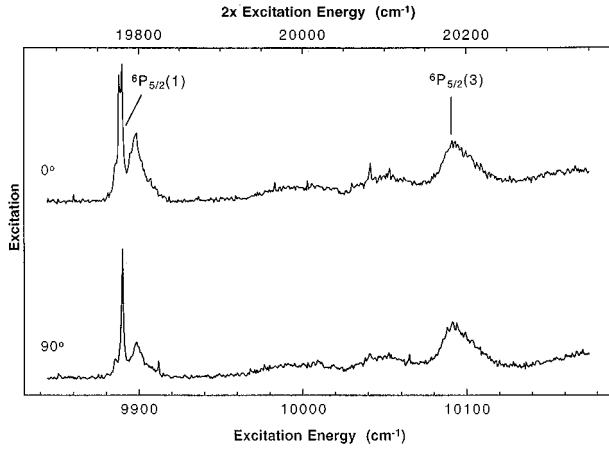


FIG. 3.  $\theta=0^\circ$  and  $\theta=90^\circ$  polarized spectra of the TPA transitions to the  ${}^6P_{5/2}$  multiplet.

### V. DISCUSSION

It is clear from Figs. 2, 4, and 6 that for most of the TPA transitions studied the calculated polarization behavior is very different from that measured experimentally, even when third-order spin-orbit corrections are included. Varying the value of  $\varphi$  between  $0^\circ$  and  $45^\circ$ , to account for any misalignment of the sample, would not result in better agreement. The transitions  ${}^8S_{7/2}(1) \rightarrow {}^6D_{7/2}(3)$ ,  ${}^8S_{7/2}(2) \rightarrow {}^6P_{5/2}(1)$ , and  ${}^8S_{7/2}(1) \rightarrow {}^6D'_{7/2}(2)$  are an exception, as they exhibit reasonable agreement between their measured polarization behavior and that predicted by the combined second- and third-order theory. All three transitions are of the  $\Gamma_n \rightarrow \Gamma_n$  type, and it is not surprising that inclusion of the third-order contribution improves the agreement obtained, as the  $(\alpha_0^0)^{\text{3rd}}$  scalar term should be important in this case. Similarly, the third-order correction improves significantly the prediction for the  ${}^8S_{7/2}(1) \rightarrow {}^6D_{7/2}(1)$  transition, which is also of this type.

Even more striking was the disagreement between the theoretical and experimentally measured values for the relative intensities of the TPA transitions investigated. The discrepancy was three orders of magnitude in some cases. Moreover, inclusion of the third-order spin-orbit correction made the discrepancy worse in most cases.

Many of the  $\text{Cm}^{3+}$  TPA transitions investigated exhibit a significant isotropic component in their intensities, apparently independent of  $\theta$ , which is not predicted by either the

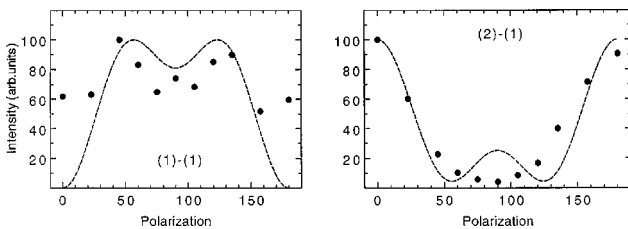


FIG. 4. Experimental polarization behavior (dots) of the  ${}^8S_{7/2} \rightarrow {}^6P_{5/2}$  two-photon absorption transitions. The second-order (dashed line) calculated polarization dependences are shown on different arbitrary scales. There are no third-order corrections for these two transitions.

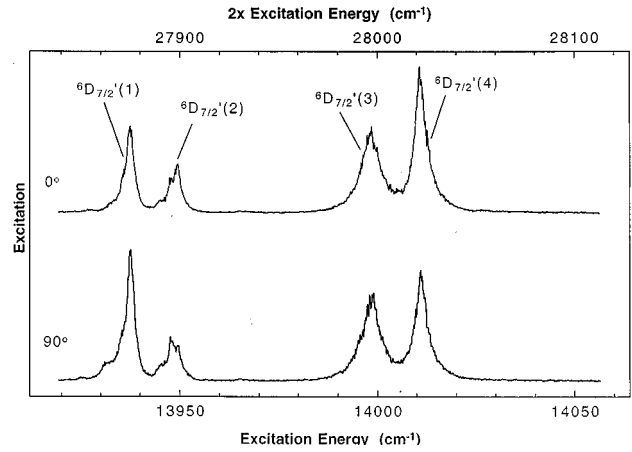


FIG. 5.  $\theta=0^\circ$  and  $\theta=90^\circ$  polarized spectra of the TPA transitions to the  ${}^6D'_{7/2}$  multiplet.

second- or third-order theories. Similar isotropy has been reported for  $\text{Eu}^{3+}$  TPA transitions in  $\text{Eu}(\text{OH})_3$  and  $\text{Eu}^{3+}:\text{LuPO}_4$ .<sup>17,18</sup> It was found that this isotropy could be accounted for phenomenologically by adding a positive constant to the polarization-dependent functions for the TPA intensities. This would correspond to an additional imaginary term in the transition matrix elements, which is independent of the polarization angles. Hence these new polarization-dependent functions for the  $\text{Cm}^{3+}$  ion have the form

$$A + B \sin^4 \theta + C \sin^2 2\theta \quad (\text{for } \Gamma_6 \leftrightarrow \Gamma_7 \text{ transitions}),$$

$$A_n + (B_n \cos^2 \theta + C_n)^2 + D_n \sin^2 2\theta$$

$$(\text{for } \Gamma_n \leftrightarrow \Gamma_n \text{ transitions}), \quad (13)$$

where  $A$ ,  $B$ ,  $C$ ,  $A_n$ ,  $B_n$ ,  $C_n$ , and  $D_n$  are positive real-valued fitting parameters. Fits to these modified functions are shown for the four  ${}^8S_{7/2} \rightarrow {}^6D_{7/2}$  transitions in Fig. 7. Of the total of ten transitions investigated, all those whose calculated polarization behavior had been in poor agreement with experiment exhibited comparatively good fits to these modified functions. For the other three transitions, the agreement with experiment was also improved. Some of this improvement may be attributable to the fact that the parameters for these functions were fitted to the experimental intensities, rather than calculated from the wave functions of the crystal-field states.

Other mechanisms may contribute to the  $\text{Cm}^{3+}$  TPA transitions, particularly that arising from the third-order crystal-field interaction. No third-order crystal-field corrections were calculated because the odd crystal-field parameters  $B_q^k$  are unknown. Such mechanisms might be responsible for discrepancies between the measured and predicted transition intensities. It is perhaps significant that the single-photon transitions were only weakly polarized for  $\text{Cm}^{3+}$  in  $\text{LuPO}_4$ .<sup>2,3</sup>

### VI. CONCLUSIONS

Two-photon absorption transitions originating from the nominally  ${}^8S_{7/2}$  ground multiplet of  $\text{Cm}^{3+}$  ions in  $\text{LuPO}_4$

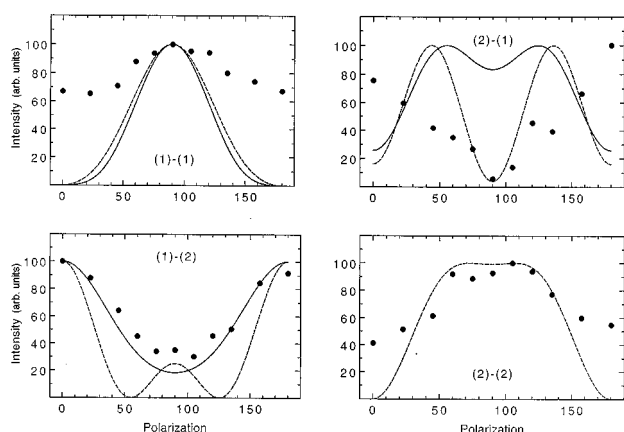


FIG. 6. Experimental polarization behavior (dots) of the  ${}^8S_{7/2} \rightarrow {}^6D'_{7/2}$  two-photon absorption transitions. The second-order (dashed line) and combined second- and third-order (solid line) calculated polarization dependences are shown on different arbitrary scales.

have been investigated. Measurement of transitions between individual crystal-field levels was possible due to the large  $9.5 \text{ cm}^{-1}$  splitting of this multiplet for the  $\text{Cm}^{3+}$  ion, compared to the splittings of less than  $1 \text{ cm}^{-1}$  for the  $\text{Gd}^{3+}$  and  $\text{Eu}^{2+}$  ions. The polarization dependences of most of these transitions could not be accounted for by the standard second-order theory, even when third-order corrections involving spin-orbit interactions within the  $5f^6-6d$  lowest excited configuration are taken into account. Addition of an imaginary constant in the expression for the amplitude improved the agreement for all of the transitions investigated. The physical mechanism to explain this additional contribution has not yet been identified. Better agreement with the observed intensities might be obtained if the third-order

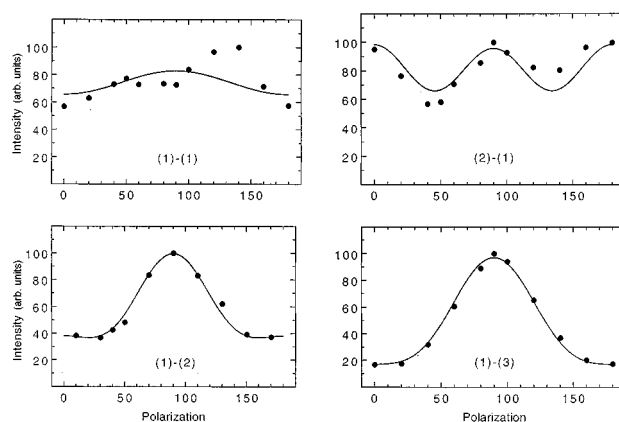


FIG. 7. Modified polarization dependences (solid line), derived from transition matrix elements which include an additional imaginary term, fitted to the experimental polarization behavior (dots) of the  ${}^8S_{7/2} \rightarrow {}^6D_{7/2}$  two-photon absorption transitions.

crystal-field corrections could be calculated and included in the polarization-dependent functions.

#### ACKNOWLEDGMENTS

Dr. M. M. Abraham and Dr. L. A. Boatner of Oak Ridge National Laboratory are gratefully acknowledged for growing and providing the crystal used for this work. This research was sponsored in part by the Director, Office of Energy Research, Office of Basic Energy Sciences, Chemical Sciences Division of the U.S. Department of Energy under Contract No. De-AC03-76SF00098 with the University of California. Partial support by NATO under Contract No. CRG 9190902 is gratefully acknowledged. The authors are indebted for the use of the  ${}^{248}\text{Cm}$  to the Division of Chemical Sciences, Office of Basic Energy Sciences, through the transplutonium element production facilities at Oak Ridge National Laboratory.

<sup>1</sup>W. K. Kot, N. M. Edelstein, M. M. Abraham, and L. A. Boatner, *Phys. Rev. B* **48**, 12 704 (1993).

<sup>2</sup>J. Sytsma, K. M. Murdoch, N. M. Edelstein, L. A. Boatner, and M. M. Abraham, *Phys. Rev. B* **52**, 12 668 (1995).

<sup>3</sup>K. M. Murdoch, N. M. Edelstein, L. A. Boatner, and M. M. Abraham, *J. Chem. Phys.* **105**, 2539 (1996).

<sup>4</sup>M. Dagenais, M. C. Downer, R. Neumann, and N. Bloembergen, *Phys. Rev. Lett.* **46**, 561 (1981).

<sup>5</sup>M. C. Downer, A. Bivas, and N. Bloembergen, *Opt. Commun.* **41**, 335 (1982).

<sup>6</sup>B. Jacquier, Y. Salem, C. Linares, J. C. Gâcon, R. Mahiou, and R. L. Cone, *J. Lumin.* **38**, 258 (1987).

<sup>7</sup>B. Jacquier, J. C. Gâcon, Y. Salem, C. Linares, and R. L. Cone, *J. Phys. Condens. Matter.* **1**, 7385 (1989).

<sup>8</sup>M. C. Downer, C. D. Cordero-Montalvo, and H. Crosswhite, *Phys. Rev. B* **28**, 4931 (1983).

<sup>9</sup>J. D. Axe, *Phys. Rev.* **136**, A42 (1964).

<sup>10</sup>B. R. Judd and D. R. Pooler, *J. Phys. C* **15**, 591 (1982).

<sup>11</sup>M. C. Downer and A. Bivas, *Phys. Rev. B* **28**, 3677 (1983).

<sup>12</sup>A. D. Nguyen, *Phys. Rev. B* **55**, 5786 (1997).

<sup>13</sup>L. A. Boatner, G. W. Beall, M. M. Abraham, C. B. Finch, R. J. Floran, P. G. Huray, and M. Rappaz, *Management of Alpha-Contaminated Wastes* (International Atomic Energy Agency, Vienna, 1981), p. 114.

<sup>14</sup>M. Rappaz, L. A. Boatner, and M. M. Abraham, *J. Chem. Phys.* **73**, 1095 (1980).

<sup>15</sup>J. C. Gâcon, J. F. Marcerou, M. Bouazaoui, B. Jacquier, and M. Kibler, *Phys. Rev. B* **40**, 2070 (1989).

<sup>16</sup>P. C. Becker, Ph.D. thesis, UC Berkeley, 1986.

<sup>17</sup>R. Mahiou, J. C. Gâcon, B. Jacquier, and R. L. Cone, *J. Lumin.* **60&61**, 664 (1994).

<sup>18</sup>J. C. Gâcon, M. Bouazaoui, B. Jacquier, M. Kibler, L. A. Boatner, and M. M. Abraham, *Eur. J. Solid State Inorg. Chem.* **28**, 113 (1991).